

1 **Supplementary for**

2 **Distinct Impacts of El Niño-Southern Oscillation and Indian Ocean Dipole**  
3 **on China's Gross Primary Production**

4 Ran Yan<sup>1,2</sup>, Jun Wang<sup>1,2\*</sup>, Weimin Ju<sup>1,2\*</sup>, Xiuli Xing<sup>3</sup>, Miao Yu<sup>4</sup>, Meirong Wang<sup>4</sup>, Jingye Tan<sup>1,2</sup>, Xunmei

5 Wang<sup>1,2</sup>, Hengmao Wang<sup>1,2</sup>, Fei Jiang<sup>1,2</sup>

6 <sup>1</sup>Frontiers Science Center for Critical Earth Material Cycling, International Institute for Earth System  
7 Science, Nanjing University, Nanjing, Jiangsu 210023, China

8 <sup>2</sup>Jiangsu Provincial Key Laboratory of Geographic Information Science and Technology, Key  
9 Laboratory for Land Satellite Remote Sensing Applications of Ministry of Natural Resources, School  
10 of Geography and Ocean Science, Nanjing University, Nanjing, Jiangsu 210023, China

11 <sup>3</sup>Department of Environmental Science and Engineering, Fudan University, No. 2005, Songhu Road, Yangpu  
12 District, Shanghai 200438, China

13 <sup>4</sup>Joint Center for Data Assimilation Research and Applications/Key Laboratory of Meteorological  
14 Disaster, Ministry of Education/Joint International Research Laboratory of Climate and Environment  
15 Change (ILCEC)/ Collaborative Innovation Center ON Forecast and Evaluation of Meteorological  
16 Disasters, Nanjing University of Information Science and Technology, Nanjing 210044, China

17 Corresponding author: Jun Wang ([wangjun@nju.edu.cn](mailto:wangjun@nju.edu.cn)); Weimin Ju ([juweimin@nju.edu.cn](mailto:juweimin@nju.edu.cn))

18

19 **Method**

20 Building on the methodology introduced by Ahlstrom et al. [2015], we incorporate an index that  
21 evaluates individual geographic locations based on their consistency, over time, in mirroring the sign  
22 and magnitude of the national GPP. For each geographical division  $j$ , its contribution to the national  
23 GPP anomaly is defined as:

24 
$$f_j = \frac{\sum_t \frac{x_{jt} |X_t|}{X_t}}{\sum_t |X_t|}$$

25 where  $x_{jt}$  is the GPP anomaly for region  $j$  at season  $t$  (SON(y0), DJF(y0), MAM(y1) and JJA(y1)),  
26 and  $X_t$  is the national GPP anomaly, such that  $X_t = \sum_t x_{jt}$ . By this definition  $f_j$  is the average relative  
27 anomaly  $x_{jt}/X_t$  for region  $j$ , weighted with the absolute national anomaly  $|X_t|$ .

28

29 Table S1. Information for the 7 sites used for verification. Where, P represents average annual  
30 precipitation, T represents average annual temperature, and PFT represents plant functional  
31 types.

<b>Site Name</b>	<b>Lat (°N)</b>	<b>Lon (°E)</b>	<b>P (mm)</b>	<b>T (°C)</b>	<b>PFT</b>	<b>years</b>
Xishuangbanna (BN)	21.93	101.27	737.1	19.40	Forest	2003~2010
Qianyanzhou (QYZ)	26.74	115.06	583.70	17.74	Forest	2003~2010
Changbaishan (CB)	42.40	128.10	234.33	3.65	Forest	2003~2010
Dinghushan (DHS)	23.17	112.53	729.09	20.12	Forest	2003~2010
Haibei Shrub (HBS)	37.67	101.33	236.33	-1.26	Shrub	2003~2010
Dangxiong (DX)	30.50	91.07	220.85	2.72	Grass	2004~2010
Yingke (YK)	38.85	100.42	31.71	7.40	Crop	2008~2010

32

33

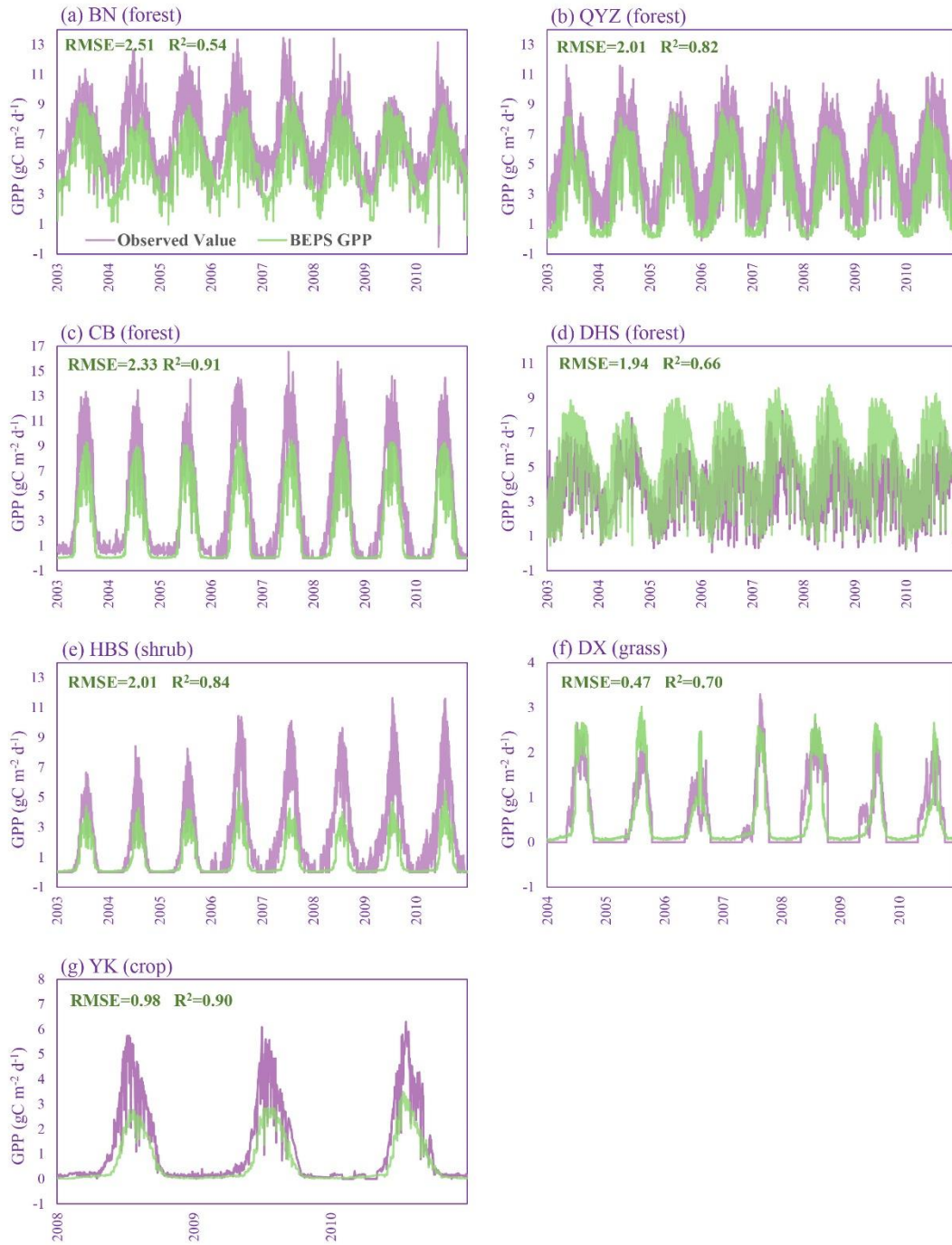
34 Table S2. Contributions of different regions to the national GPP changes in different events.

	Southern	Northern	Northwest	TP
El Niño	59.58%	27.29%	4.47%	8.66%
La Niña	76.21%	27.96%	0.46%	-4.64%
pIOD	53.65%	31.67%	6.88%	7.79%
nIOD	37.25%	46.99%	7.48%	8.28%

35

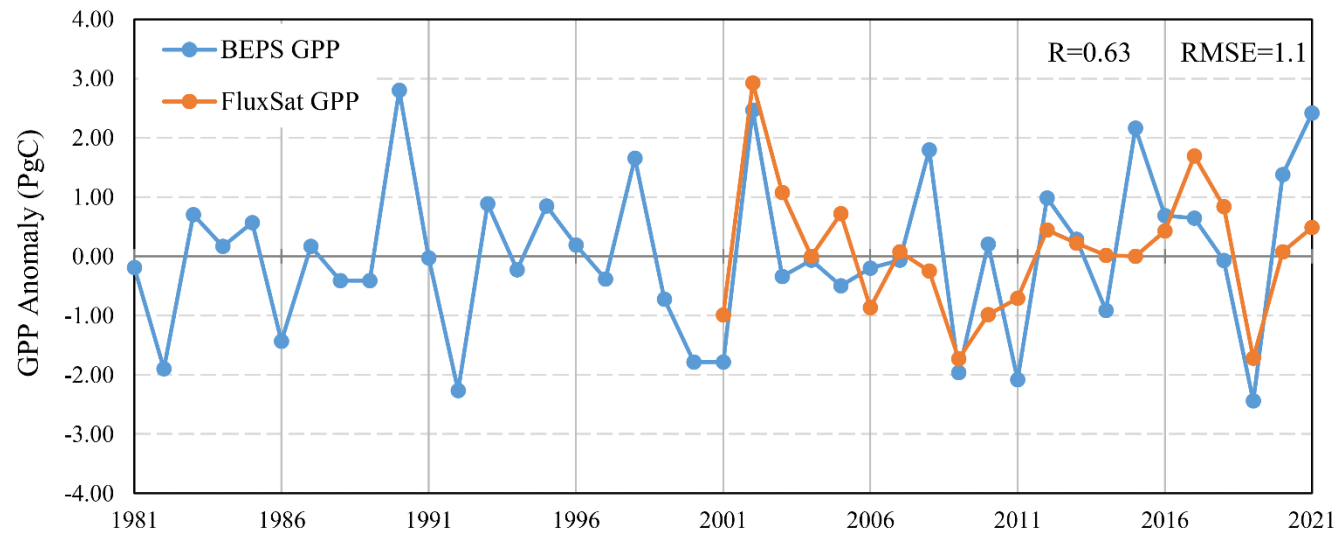
36 Table S3. Total GPP anomaly ( $\text{Tg C yr}^{-1}$ ) at the provincial scale for different events. The province names  
 37 are abbreviated and sorted alphabetically.

Province	El Niño	La Niña	pIOD	nIOD
Anhui	-8.98	17.62	-6.89	13.55
Beijing	-0.62	-0.60	0.37	-0.83
Chongqing	9.25	-0.11	2.31	-2.31
Fujian	-1.96	6.48	-87.99	21.44
Gansu	0.20	-1.30	15.98	-13.44
Guangdong	16.69	-9.21	-78.31	11.21
Guangxi	0.19	-9.25	-92.87	-1.30
Guizhou	-8.18	3.75	-25.69	-2.18
Hainan	-2.56	3.49	-26.49	8.71
Hebei	-11.93	0.94	18.49	-6.57
Henan	0.68	10.48	51.21	10.12
Heilongjiang	6.14	-20.52	44.72	-4.70
Hubei	-3.94	-0.59	-51.31	11.04
Hunan	4.90	2.80	-6.86	1.78
Jilin	-1.22	1.42	-3.87	-6.14
Jiangsu	-10.57	6.84	11.09	-2.17
Jiangxi	-8.97	8.94	-130.96	17.25
Liaoning	-9.07	14.68	-13.89	-8.73
Inner Mongolia	-23.06	25.16	-23.87	-48.72
Ningxia	0.33	-0.04	0.45	-1.72
Qinghai	0.84	-3.20	-8.07	-11.85
Shandong	-14.70	6.69	25.48	4.49
Shanxi	4.19	7.45	31.41	-6.76
Shaanxi	21.93	-3.38	40.21	-10.52
Sichuan	-16.89	-9.78	28.56	-13.36
Taiwan	-1.87	2.62	-4.72	2.58
Tianjin	-0.90	-0.34	-0.72	-0.51
Tibet	-9.98	-5.25	24.50	12.18
Xinjiang	15.27	-17.47	-5.84	9.00
Yunnan	-90.21	14.46	-112.79	48.15
Zhejiang	-3.34	4.19	-11.64	6.48



39  
40  
41

Fig. S1. Comparison between BEPS simulated and Flux Tower observed daily GPP at 7 sites.

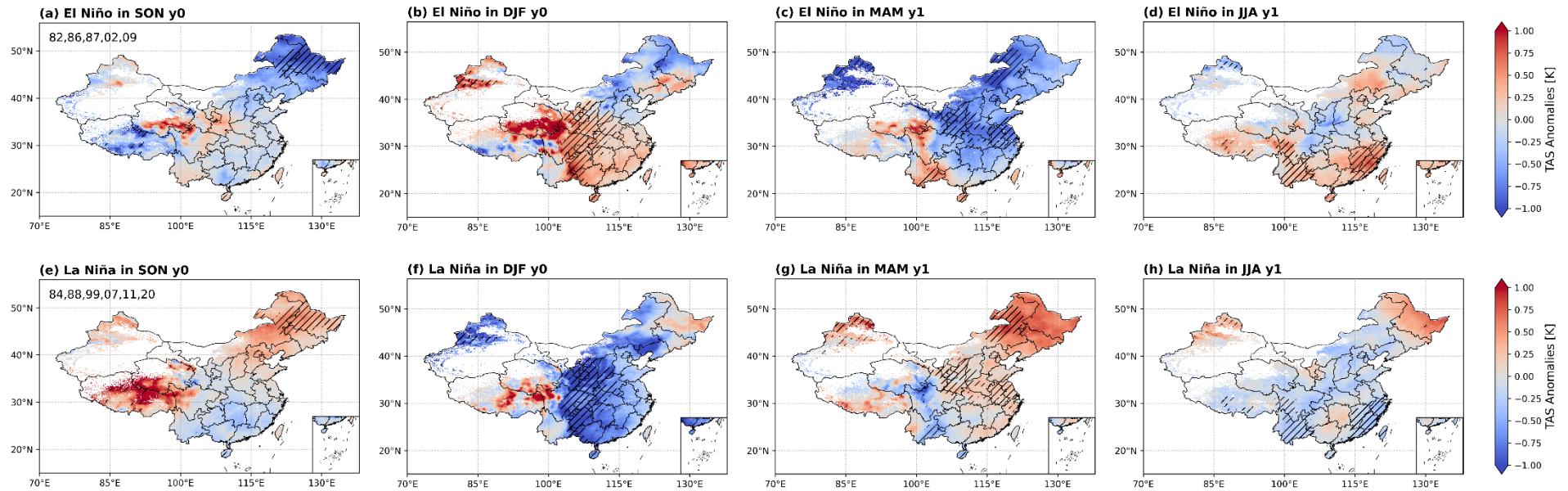


42

43

Fig. S2. Total annual gross primary productivity (GPP) anomalies in the Boreal Ecosystem Productivity Simulator (BEPS) model and FluxSat data from 1981 to 2021.

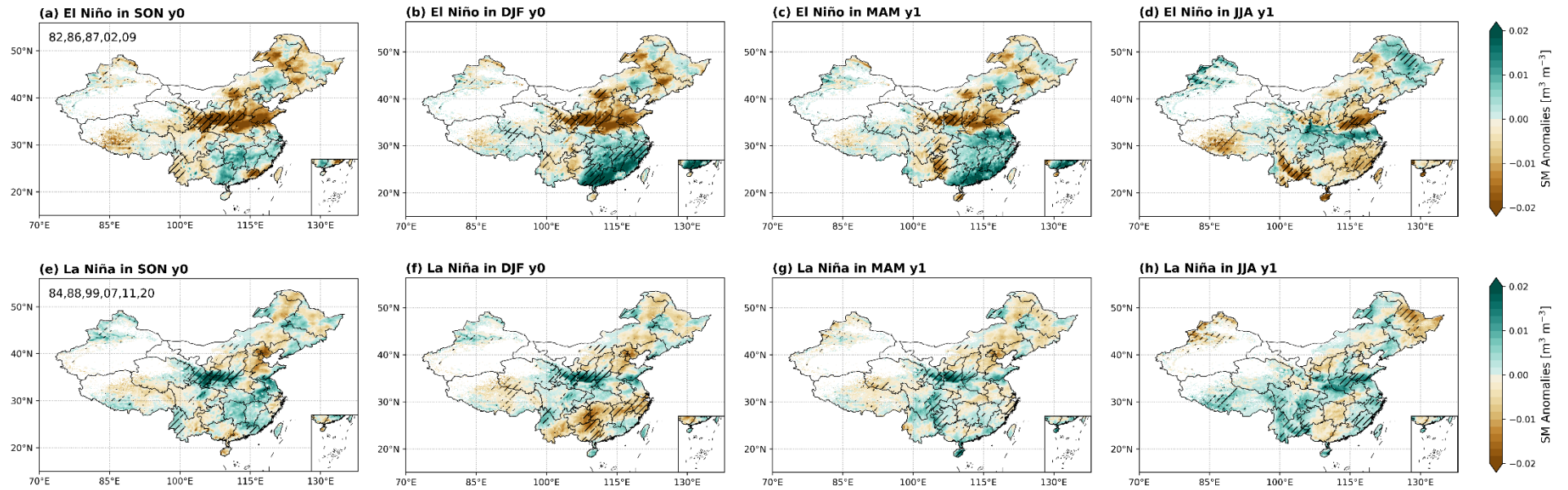
44



45

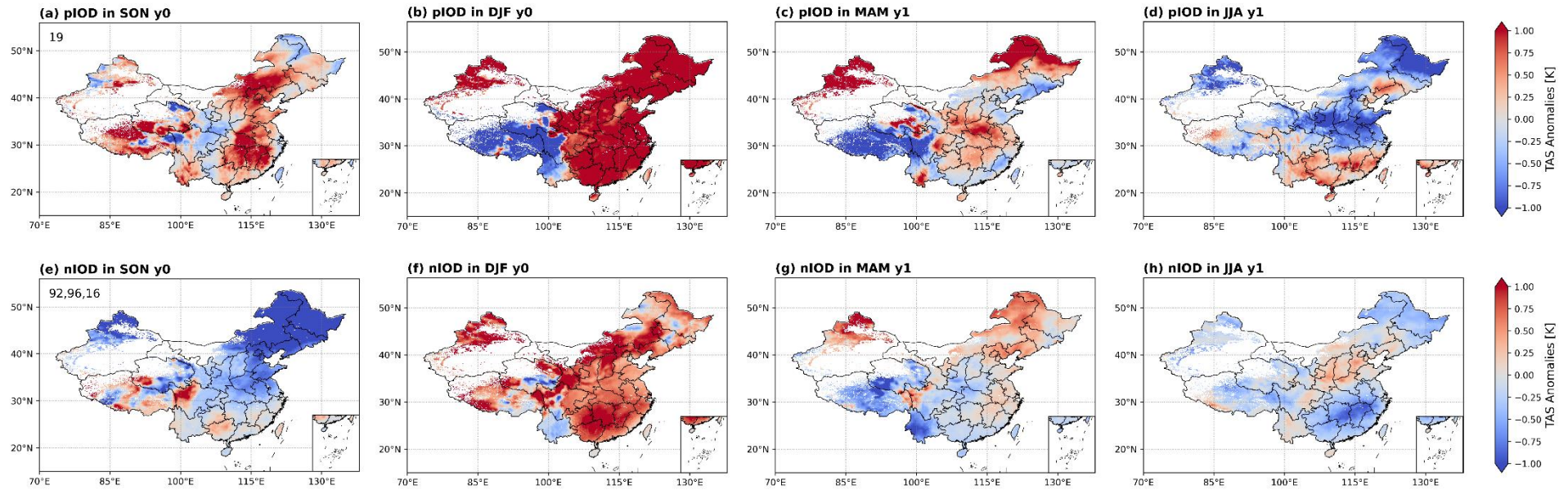
46 Fig. S3. Spatial distributions of seasonal composite surface air temperature (TAS) anomalies for ENSO events. The black slashes indicate areas where El Niño events  
 47 differ significantly from La Niña events ( $p \leq 0.05$ ) based on the Student's two-sample  $t$ -test. Numbers in subplots (first column) denote the years for composite analysis.





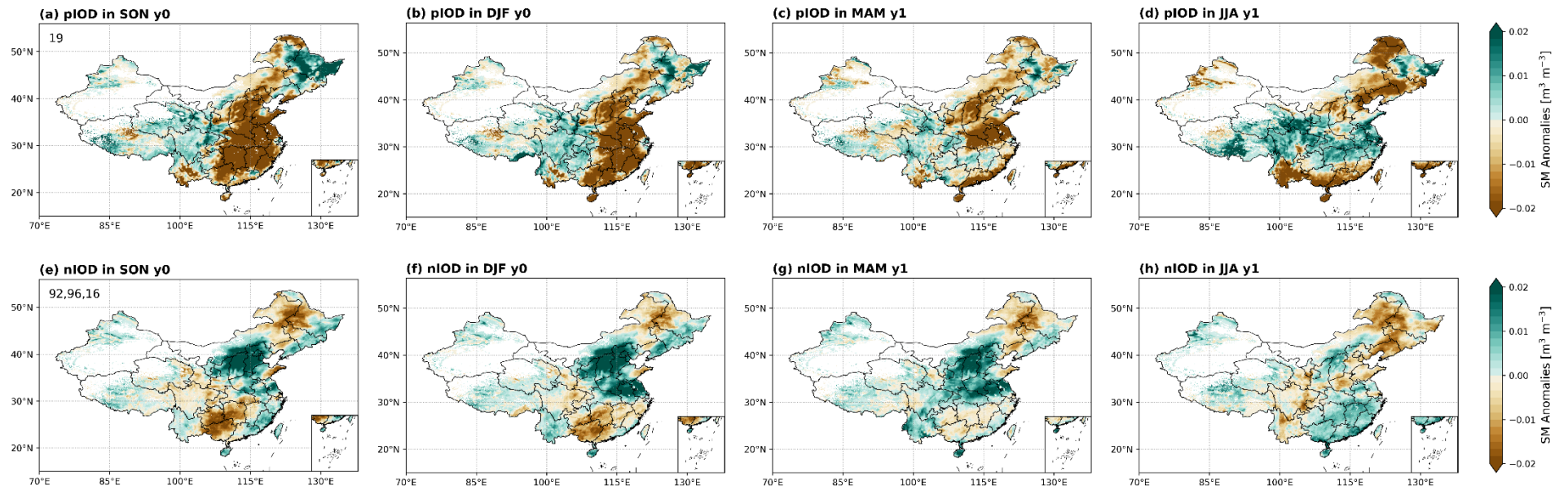
48

49 Fig. S4. Same as Fig. S2, but for soil moisture (SM).



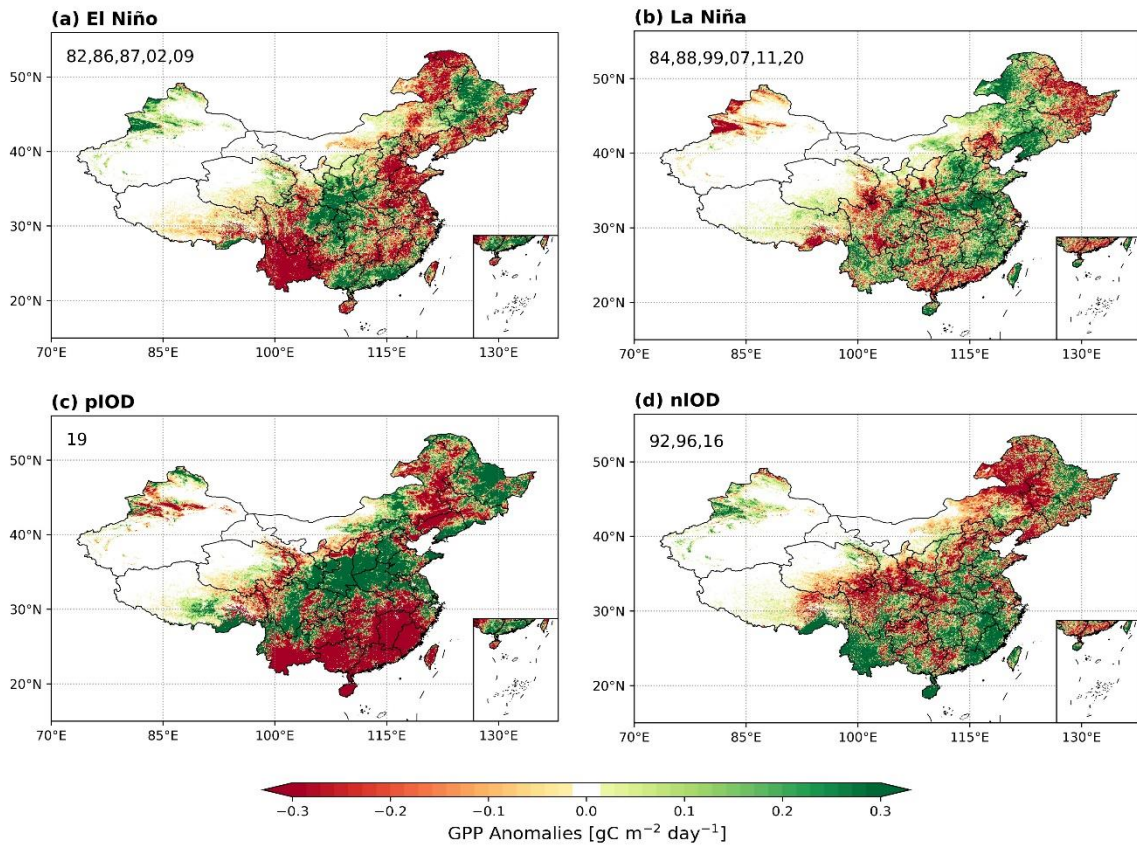
50

51 Fig. S5. Spatial distributions of seasonal composite TAS anomalies for IOD events. Numbers in subplots (first column) denote the years for composite analysis.



52

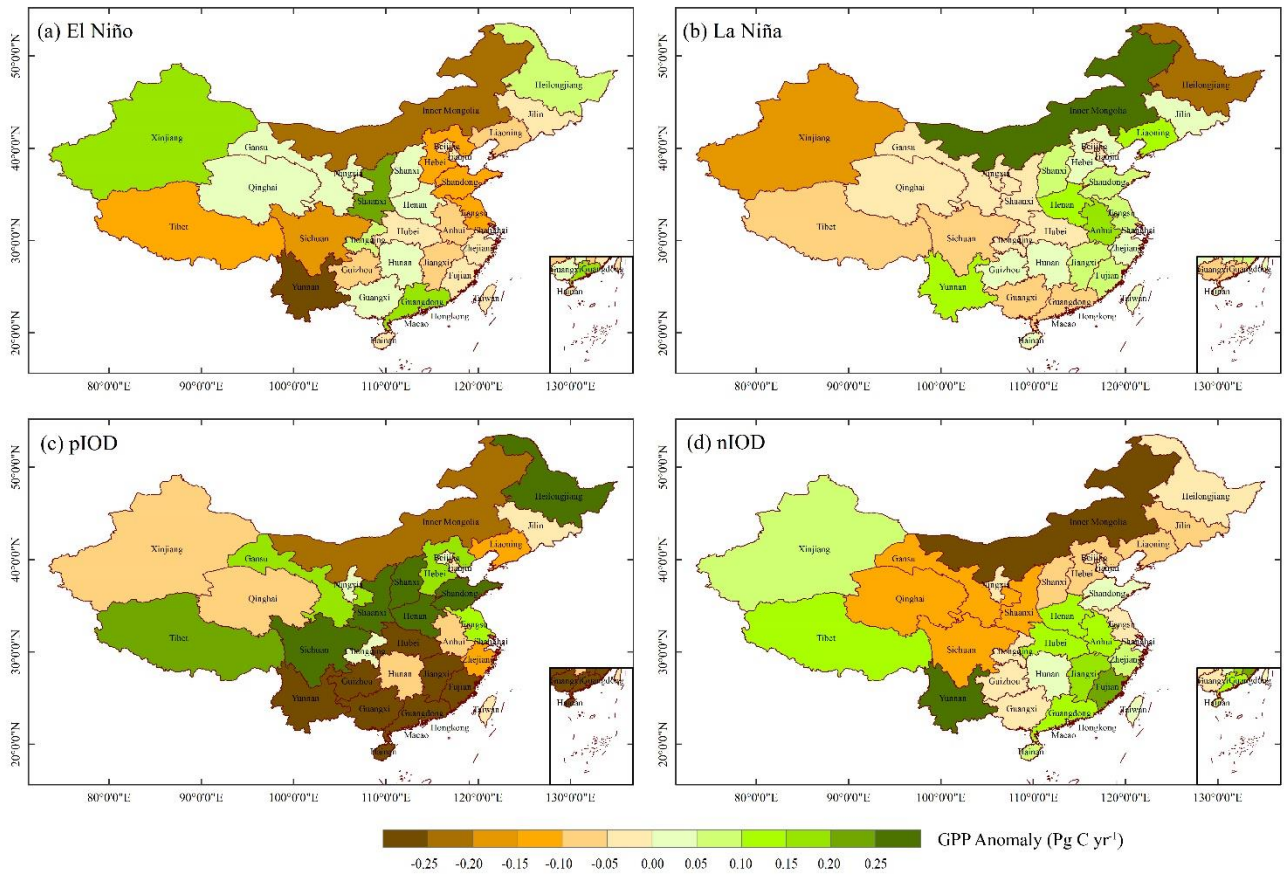
53 Fig. S6. Same as Fig. S4, but for SM.



54

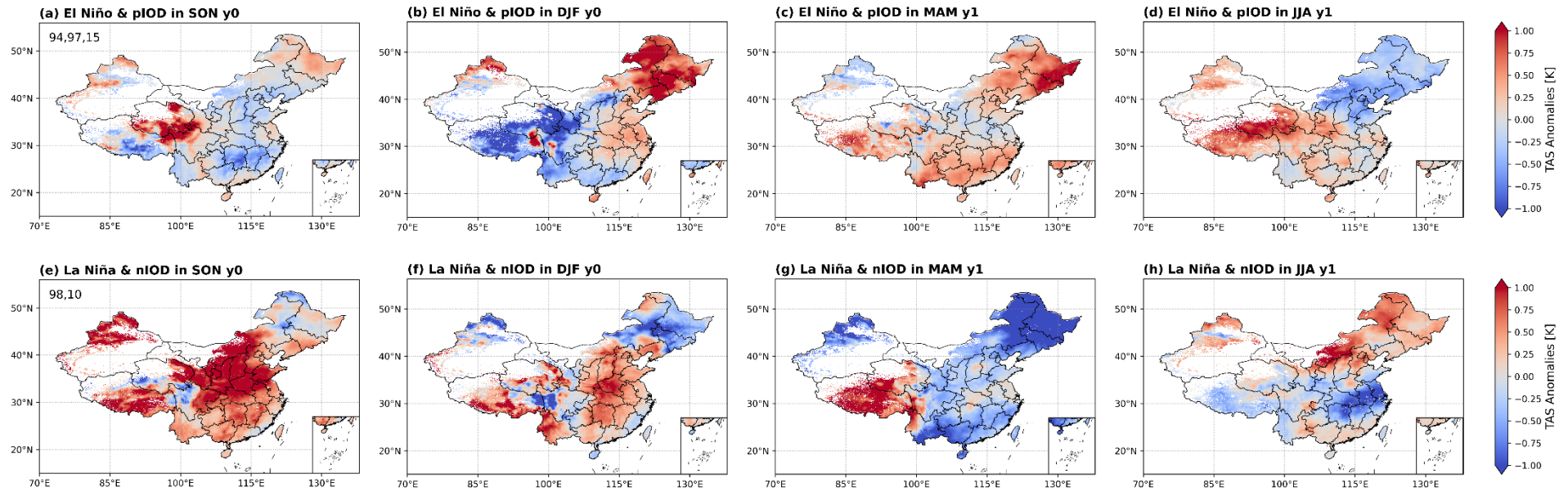
55 Fig. S7. Spatial distributions of annual mean composite GPP anomalies for different event classes. Numbers in  
 56 subplots denote the years for composite analysis.

57



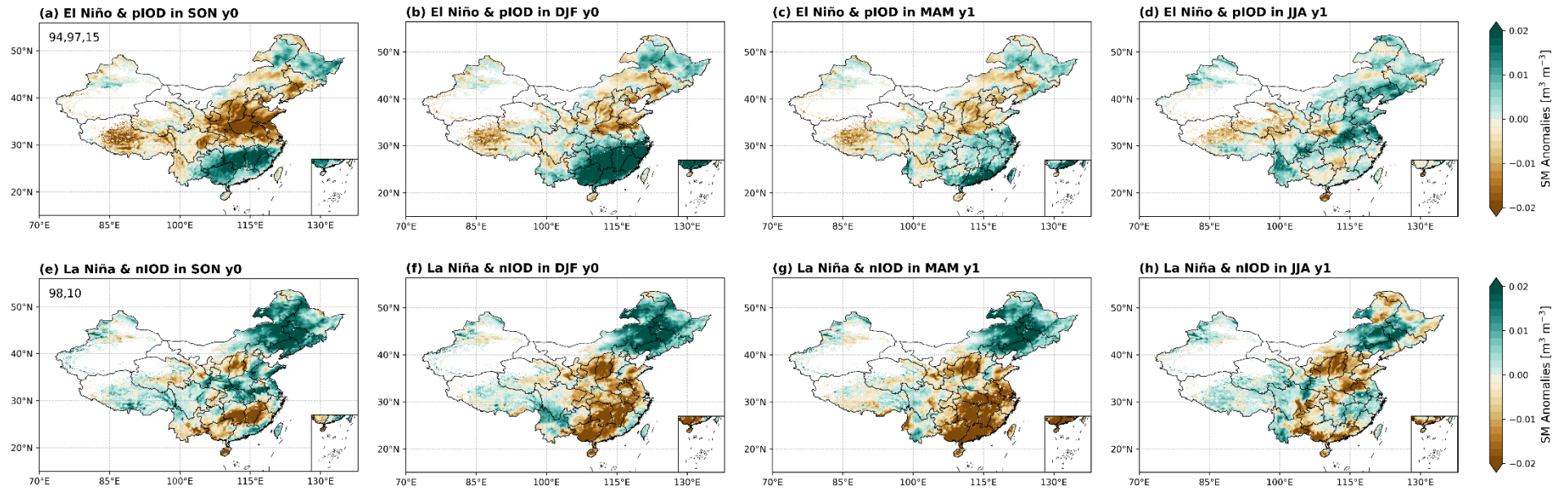
58

59 Fig. S8. Spatial distributions of total composite GPP anomalies ( $\text{Pg C yr}^{-1}$ ) at the provincial scale for different  
 60 classified events.



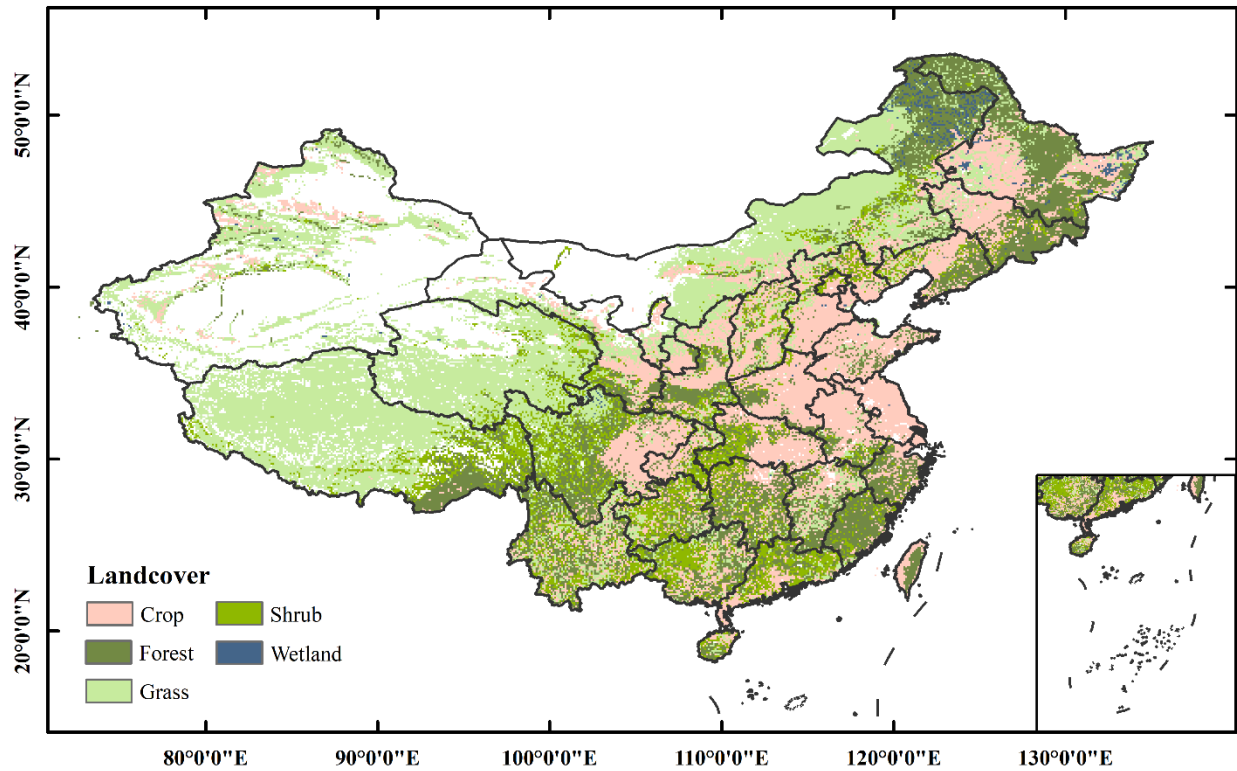
61

62 Fig. S9. Spatial distributions of seasonal composite TAS anomalies for compound events. Numbers in subplots (first column) denote the years for composite analysis.



63

64 Fig. S10. Same as Fig. S8, but for SM.



65

66 Fig. S11. Geographical distributions of landcover classes, based on the 1:1 000 000 Atlas of vegetation in China  
 67 (<https://www.resdc.cn/data.aspx?DATAID=122>). In this study, the data were resampled to  $0.1^{\circ} \times 0.1^{\circ}$  using the  
 68 area maximization method. Specifically, forest contains its needleleaf forests, broadleaf forests and mixed  
 69 forests; grass contains grassland, grass, and meadow; crop refers to cultivated vegetation, including crops and  
 70 artificial orchards and economic forests.

71



72 **Reference**

- 73 Ahlstrom, A., et al. (2015), The dominant role of semi-arid ecosystems in the trend and variability of the land  
74 CO<sub>2</sub> sink, *Science*, 348(6237), 895-899, <https://doi:10.1126/science.aaa1668>.